Clinica Chimica Acta 498 (2019) 135–142

Contents lists available at ScienceDirect

Clinica Chimica Acta

journal homepage: www.elsevier.com/locate/cca

# Plasma metabolites Xanthine, 4-Pyridoxate, and D-glutamic acid as novel potential biomarkers for pulmonary tuberculosis

Huai Huang[a,b], Li-Ying Shi[c], Li-Liang Wei[d], Yu-Shuai Han[b], Wen-Jing Yi[b], Zhi-Wen Pan[e], Ting-Ting Jiang[a], Jing Chen[b], Hui-Hui Tu[b], Zhi-Bin Li[b], Yu-Ting Hu[a,b], Ji-Cheng Li[a,b,*]

[a] School of Medicine, South China University of Technology, Guangzhou 510006, PR China
[b] Institute of Cell Biology, Zhejiang University, Hangzhou 310058, PR China
[c] Department of Clinical Laboratory, Zhejiang Hospital, Hangzhou 310013, PR China
[d] Department of Pneumology, Shaoxing Municipal Hospital, Shaoxing 312000, PR China
[e] Department of Clinical Laboratory, Zhejiang Cancer Hospital, Hangzhou 310022, PR China

ARTICLE INFO

*Keywords:*
Xanthine
D-glutamic acid
4-Pyridoxate
Potential biomarkers
Pulmonary tuberculosis
Metabolomics

ABSTRACT

*Background:* The lack of rapid and efficient diagnostic methods has been one of the most frustrating challenges in controlling the pulmonary tuberculosis (TB) epidemic. This study was aimed to identify novel non-invasive biomarkers for pulmonary TB.

*Methods:* The subjects in this study were divided into four groups: the pulmonary TB group, the community-acquired pneumonia (CAP) group, the lung cancer (LC) group, and the normal control (NC) group. Plasma small molecule metabolites were investigated in each group by using ultra-high performance liquid chromatography coupled with Q Exactive mass spectrometry. Multivariate statistical methods and bioinformatics were used to analyze the data.

*Results:* We identified three differential plasma metabolites such as, Xanthine, 4-Pyridoxate and D-glutamic acid in the pulmonary TB group, compared to the other groups (CAP, LC and NC). The pathway enrichment analysis indicated that the energy source in pulmonary TB was multi-center, which might be involved in maintaining the reproductive ability and virulence of *Mycobacterium tuberculosis.*

*Conclusion:* The results suggested that Xanthine, 4-Pyridoxate, and D-glutamic acid may serve as potential biomarkers for pulmonary TB. The present study provides experimental basis for developing potential biomarkers of pulmonary TB.

## 1. Introduction

Pulmonary tuberculosis (TB) is a chronic infectious disease caused by *Mycobacterium tuberculosis* (MTB) that most often affects the lungs. According to the recent World Health Organization (WHO) global report, there were around 10 million new TB cases and 1.6 million TB deaths in 2017. The incidence of TB is high in China [1]. In 2017, the number of new TB cases in China was about 889,000, accounting for 8.9% of the total global TB cases (2nd in the world), and there were about 37,000 TB deaths in the same year [1]. Since the launch of Directly Observed Treatment Short-Course (DOTs) strategy in 1995, the early diagnosis of TB has been recognized as the key to achieving the end of TB epidemic [2].

The current diagnostic methods are not adequate for early and

*Abbreviation:* TB, Tuberculosis; MTB, *Mycobacterium tuberculosis*; D-Glu, D-glutamic acid; UPLC-QE-MS, ultra-high performance liquid chromatography coupled with Q Exactive mass spectrometry; UPLC, ultra-high performance liquid chromatography; NC, normal controls; CAP, community-acquired pneumonia; LC, lung cancer; IDA, information-dependent basis; LC-MS, liquid chromatography tandem mass spectrometry; MS, mass spectrometry; PCA, principal component analysis; OPLS-DA, orthogonal projections to latent structures-discriminant analysis; VIP, variable importance in the projection; XO, xanthine oxidase; Th, T helper; PGN, peptidoglycan; NOD1, nucleotide-binding oligomerization domain-containing protein 1; TNF, tumor necrosis factor; IL., interleukin

* Corresponding author at: School of Medicine, South China University of Technology, 382 Waihuan East Road, University Town, Panyu District, Guangzhou 510006, PR China.

*E-mail addresses:* yichengshuian5653@163.com (H. Huang), shi-lee-ying@163.com (L.-Y. Shi), weililiang1981@163.com (L.-L. Wei), hyshuaizd@zju.edu.cn (Y.-S. Han), 18268178640@163.com (W.-J. Yi), pan-zhiwen@163.com (Z.-W. Pan), jiang_tingting1989@126.com (T.-T. Jiang), chenjing2017@zju.edu.cn (J. Chen), baiweituhuihui@163.com (H.-H. Tu), lizhibinaa@163.com (Z.-B. Li), huyuting29@163.com (Y.-T. Hu), lijichen@zju.edu.cn (J.-C. Li).

https://doi.org/10.1016/j.cca.2019.08.017
Received 2 June 2019; Received in revised form 18 August 2019; Accepted 19 August 2019
Available online 20 August 2019
0009-8981/ 

accurate diagnosis of TB. Sputum smear microscopy is only effective in diagnosing TB when the bacterial load is > 10,000 organisms per ml sputum sample, and it cannot distinguish other acid-fast staining organisms. Moreover, the sputum smear positivity rate of TB has been shown to be only 20–30% [3]. Sputum culture is considered as the gold standard for detecting MTB, but it may take 4 to 8 weeks to provide results with the positive rate of only 20–25% [2]. This may lead to delayed treatment of non-open TB patients. The sensitivity and specificity of the WHO recommended Xpert technology has been shown to be significantly reduced in the samples with low bacterial load, such as sputum-negative TB and childhood TB [4]. Therefore, there is an urgent need to develop new rapid, effective and simple biomarkers of pulmonary TB in order to control the TB epidemic.

Unlike sputum, changes in the blood of TB patients have been shown to be positively correlated with the severity of the disease, and these changes gradually disappeared after effective treatment [5]. Metabolites can be endogenous (synthesized within the human biological system) or exogenous (imported from outside) [6]. The changes in metabolites cannot be fully predicted from the knowledge of the human genome, transcriptome and proteome [7]. Therefore, metabolomics can help to further understand the interaction between MTB and the human body.

Serum samples have been used previously to detect circulating metabolic markers for TB [8–10]. However, during serum extraction, fibrinogen is converted to fibrin due to blood coagulation, resulting in a decrease in serum fibrinogen content. Our previous study found that serum fibrinogen degradation products were important for the diagnosis of TB [11]. Therefore, there is some bias in the study of biomarkers for TB based on serum samples. In addition, the internal environment of the blood that has not coagulated in the body is better reflected in plasma than in serum. In terms of plasma metabolomics of TB, Lau S K P et al. identified four differential plasma metabolites in TB patients compared with the pneumonia patients and normal controls by using liquid chromatography tandem mass spectrometry (LC-MS). They speculated that these four differential metabolites could serve as potential biomarkers for TB and constructed a diagnostic model for TB [12]. The study demonstrated the utility of plasma metabolites as potential biomarkers for TB diagnosis. However, the study lacked identifying the role of these biomarkers in differentiating TB from other lung diseases such as lung cancer. It is clinically importance to distinguish pulmonary TB from lung cancer, especially in patients with only a single TB lesion. Lung cancer often presents with clinical symptoms and imaging features similar to pulmonary TB. Therefore, metabolic changes in the plasma of pulmonary TB patients compared with lung cancer patients need to be further evaluated.

In this study, differentially abundant plasma metabolites were screened by using the ultra-high performance liquid chromatography coupled with Q Exactive mass spectrometry (UPLC-QE-MS) in pulmonary TB patients and normal controls (NC) or patients with other pulmonary diseases such as, community-acquired pneumonia (CAP) and lung cancer (LC). Metabolic pathways and potential biomarkers characterizing pulmonary TB were identified. Our study may provide experimental data for developing laboratory standards for potential biomarkers of pulmonary TB.

## 2. Materials and methods

### 2.1. Ethics and clinical subjects

This study was performed in compliance with the Declaration of Helsinki. The study was approved by the Ethics Committee of the Zhejiang University Medical Department, China. Written informed consent was obtained from all subjects prior to blood sample collection.

A case-control study was designed and plasma samples were collected for metabolomics analysis. Pulmonary TB patients were diagnosed according to the diagnostic criteria for pulmonary TB of the National Health Commission of the People's Republic of China [13]. All patients met one of the following pulmonary TB diagnostic criteria: 1. positive sputum examinations (smear or culture); 2. negative sputum examinations and chest X-ray or CT scan revealing evidences typical of active TB; 3. pathological diagnosis of TB in lung specimens; 4. suspected pulmonary TB after clinical follow-up and X-ray or CT scan observations after excluding other pulmonary diseases; 5. clinical elimination of other causes of pleural effusion and diagnosis of tuberculosis pleurisy. Diagnostic criteria for CAP was based on the guidelines for primary care of adult community acquired pneumonia of China [14]: 1. Community morbidity; 2. Clinical manifestations related to pneumonia: ① newly developed symptoms of cough with or without purulent sputum, chest pain, dyspnea and hemoptysis, ② fever, ③ abnormal chest sounds on auscultation, ④ peripheral white blood cell count > $10 \times 10^9$/L or < $4 \times 10^9$/L, with or without left shift; 3. chest X-ray or CT scan revealing findings including new patchy infiltrates, segmental changes, or interstitial changes with or without pleural effusion. Criteria 1 and 3 plus any of the findings in criteria 2, except for pulmonary TB, lung cancer, non-infectious pulmonary interstitial disease, pulmonary edema, atelectasis, pulmonary embolism, pulmonary eosinophilic infiltration and pulmonary vasculitis. Patients with LC were diagnosed by histopathology combined with immunohistochemistry of lung lesions. The normal controls (NC) were healthy subjects. Patients with extra-pulmonary TB, chronic disease, extra-pulmonary malignancies, HIV infection or autoimmune disease were excluded from the study.

A total of 136 heparin anti-coagulated plasma samples were collected from all participants between August 2013 and August 2018 including 35 pulmonary TB samples from the Shaoxing Municipal Hospital (China), 35 NC samples from the Zhejiang Hospital (China), 35 CAP samples from the Zhejiang People's Hospital (China), and 31 LC samples from the Zhejiang Cancer Hospital (China). Demographic analysis showed no statistically significant difference in age and gender between the groups (Table 1).

### 2.2. Collection of plasma samples and extraction of metabolites

Blood samples were collected from all subjects prior to the start of the treatment. Morning fasting blood samples were drawn and centrifuged at 4 °C, 3000 r/min for 10 min. The supernatant was aspirated, and frozen at −80 °C.

The frozen heparin anti-coagulated plasma samples were thawed on ice and 100 μl of each sample was transferred to a 1.5 ml sterile microcentrifuge tube. After the addition of 300 μl of methanol (containing internal standard L-2-chlorophenylalanine 1 μg/ml), each sample was vortexed for 30 s, sonicated for 10 min in ice-water bath, and incubated for 1 h at −20 °C to precipitate proteins. Then each sample was centrifuged at 12000 rpm for 15 min at 4 °C [15]. The resulting supernatants were transferred to LC-MS vials and stored at −80 °C until the UPLC-QE-MS analysis. Each quality control sample was also prepared by mixing an equal aliquot of the supernatants from each sample. The treatment methods were the same as above.

### 2.3. LC-MS/MS analysis

With the ultra-high performance liquid chromatography (UPLC) HSS T3 column (2.1 mm × 100 mm, 1.8 μm), the LC-MS/MS analysis was performed using the UPLC system (1290, Agilent Technologies, USA) coupled with Q Exactive (Orbitrap MS, Thermo, Germany). The mobile phase A: for positive, it was 0·1% formic acid in water, and 5 mmol/l ammonium acetate in water for negative. The mobile phase B: it was acetonitrile. The elution gradient was set as follows: 0 min, 99% A; 1 min, 99% A; 8 min, 1% A; 10 min, 1% A; 10.1 min, 99% A; 12 min, 99% A. The flow rate was 0.5 ml/min and the injection volume was 2 μl. During the LC/MS experiment, the Q Exactive mass spectrometer was used for acquiring the MS/MS spectra on the information-dependent

**Table 1**
Characteristics of the pulmonary TB patients, CAP patients, LC patients and normal controls.

| | TB Patients (N = 35) | Normal Controls (N = 35) | CAP Patients (N = 35) | LC Patients (N = 31) | P-Value |
|---|---|---|---|---|---|
| Age, years range (Median ± IQR) | 18–64 (41.00 ± 23.00) | 23–60 (46.00 ± 16.00) | 15–64 (46.00 ± 22.00) | 28–64 (53.00 ± 10.00) | 0.0712[a] |
| Gender Female, no. (%) | 17 (48.57) | 11(31.43) | 12 (34.29) | 12 (38.71) | 0.4745[b] |
| Sputum smear: Positive, no. (%) | 30(85.71) | / | / | / | / |
| Lung lesion: Single/double | 19/16 | / | / | / | / |
| Chest X-ray: Cavity, no. (%) | 6 (17.14) | / | / | / | / |

N: number of subjects; TB: pulmonary tuberculosis; CAP: community acquired pneumonia; LC: lung cancer.
[a] P-value among four groups from Kruskal-Wallis H test.
[b] P-value among four groups from the chi-square test.

basis (IDA). Depending on preselected criteria, the acquisition software (Xcalibur 4.0.27, Thermo) continuously evaluated the full scan survey MS data when it collected and triggered the acquisition of MS/MS spectra in this mode. ESI source conditions were set as following: Sheath gas flow rate was 45 Arb, Aux gas flow rate was 15Arb, Capillary temperature at 320 °C, Full ms resolution was 70,000, MS/MS resolution was 17,500, Collision energy was 20/40/60 eV in NCE model, Spray Voltage was 3.8 kV for positive or −3.1 kV for negative, respectively [16].

### 2.4. Data processing and statistical analysis

MS raw data (.RAW) files were converted to the .mzML format by Proteo Wizard, and normalization were processed by R package XCMS (version 3.2). The retention time (RT), mass-to-charge ratio (*m/z*) values, and peak intensity were consisted in the generated data matrix of the preprocessed results. The peak after XCMS data processing was annotated with in-house MS/MS database by OSI-SMMS (version 1.0, Dalian Chem Data Solution Information Technology Co. Ltd.).

Multivariate statistical analyses were conducted using the SIMCA software (V14.1, Sartorius Stedim Data Analytics AB, Umea, Sweden). The data were subjected to logarithmic (LOG) conversion plus centralization (CTR) formatting and UV formatting processing, and then automatically modeled. Principal component analysis (PCA) was performed first, followed by the orthogonal projections to latent structures-discriminant analysis (OPLS-DA) for the first principal component. The model quality was tested using a seven-fold cross validation. In addition, the parameters $R^2Y$ (the interpretability of the model for the categorical variable Y) and $Q^2$ (predictability of the model) were used to evaluate the validity of the model. Finally, through the permutation test, the order of the categorical variables Y was randomly changed multiple times to obtain different random $Q^2$ values to further test the validity of the model [17].

Statistical analysis was performed using SPSS software (SPSS 18.0, Chicago, IL, USA). Parametric data were tested by Student's *t*-test and chi-square test for the composition ratios. Nonparametric analysis was carried out using the Mann-Whitney *U* test for two groups and Kruskal-Wallis H test for three or more groups. The two-tailed P values < 0.05 were considered statistically significant. Metabolic pathways were analyzed by the Kyoto Encyclopedia of Genes and Genomes pathway database (https://www.kegg.jp/kegg/pathway.html). Scatter plots were drawn using GraphPad Prism 5 software.

## 3. Results

### 3.1. Raw mass spectrometry data preprocessing

By using UPLC-QE-MS, the MS data of 136 heparin anti-coagulated plasma samples in four experimental groups were labeled. After baseline filtering, peak identification, integration, retention time correction, peak alignment and normalization, 3973 and 4043 peak characteristics were detected, respectively, in the positive and negative spectral modes.

In order to separate the important features of significant differences between TB and non-TB groups, the OPLS-DA model was established and the variable importance in projection (VIP) value of each feature was obtained. First, the reliability of the OPLS-DA model was evaluated. The OPLS-DA score plots showed that the characteristics of metabolite were able to clearly distinguish the TB group from the NC group, the CAP group, and the LC group (Fig. 1). The permutation test showed that the performance of OPLS-DA model data was consistent with that of the standard parameters (Table 2). Moreover, the OPLS-DA model exhibited a good robustness and no over-fitting (Supplementary Fig. 1). Therefore, it can be effectively and reliably applied to biomarker screening.

### 3.2. Identification of plasma metabolites

The Student's *t*-test was used to determine the difference between groups (TB/NC groups, TB/CAP groups, and TB/LC groups) for the features in which the VIP value was > 1 in the OPLS-DA model. And features that satisfied $p < 0.05$ and VIP > 1 were filtered out. Between the TB/NC groups, 1024 features were screened by positive spectra and 1362 features by negative spectra; between the TB/CAP groups, 752 features were screened by positive spectra and 771 by negative spectra; between the TB/LC groups, 940 features were screened by positive spectra and 1048 features by negative spectra. The results were displayed in the form of volcano plots (Fig. 2).

The differentially abundant metabolites were further identified by MS/MS spectrum matching ($p < 0.05$, and VIP > 1.2) (Supplementary Tables 1, 2, 3). Among them, 60 differentially abundant metabolites (17 up-regulated and 43 down-regulated metabolites) were identified between the TB group and the NC group, 38 differentially abundant metabolites (25 up-regulated and 13 down-regulated metabolites) were identified between the TB group and the CAP group, and 53 differentially abundant metabolites (14 up-regulated and 39 down-regulated metabolites) were identified between the TB group and the LC group.

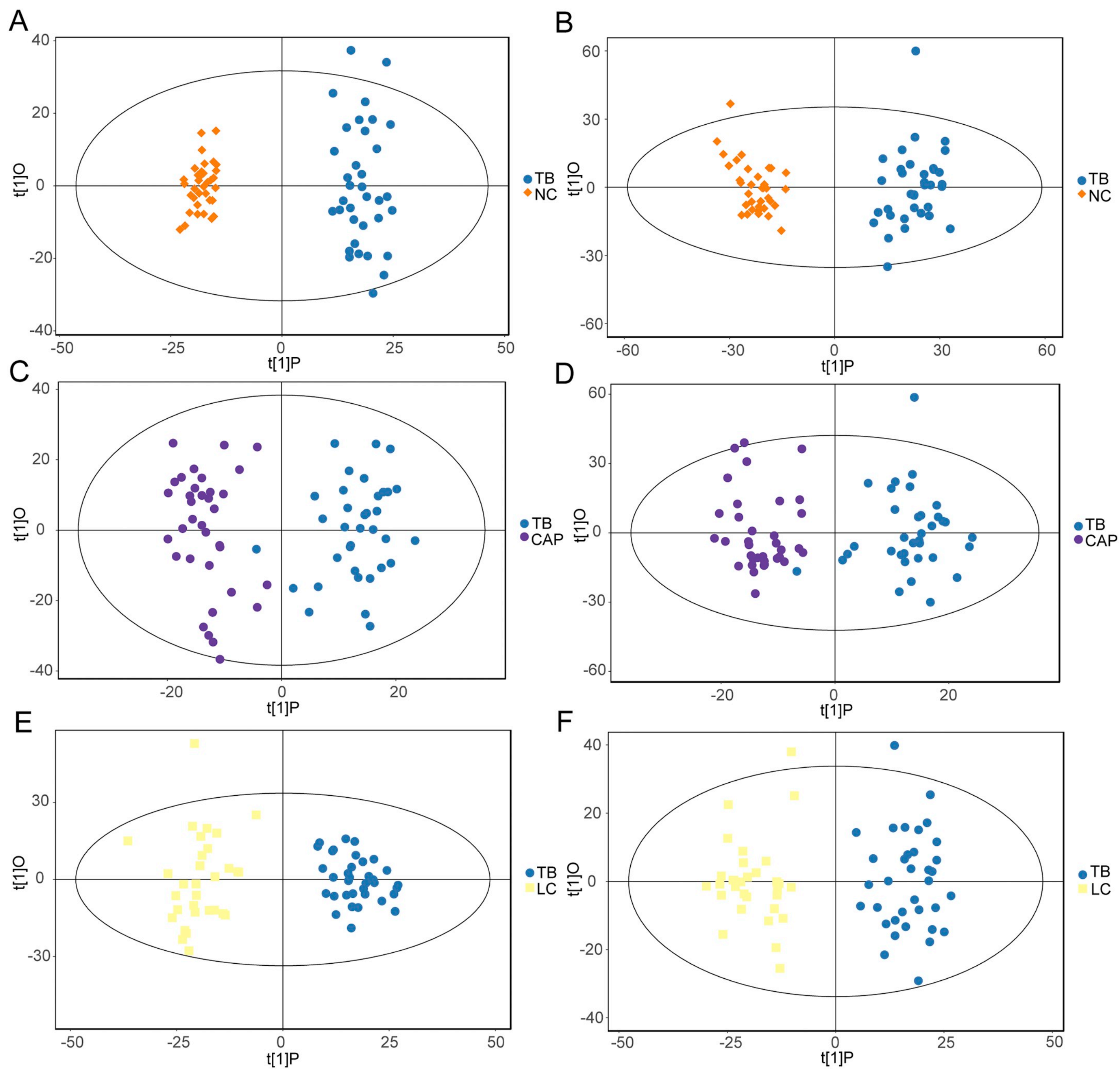


**Fig. 1.** The OPLS-DA models. For the TB/NC group in positive (A) and negative (B) ion mode, for the TB/CAP group in positive (C) and negative (D) ion mode, for the TB/LC group in positive (E) and negative (F) ion mode.

**Table 2**
Permutation test results of the OPLS-DA models.

| | Ion mode | $R^2X$ | $R^2Y$ | $Q^2$ |
|---|---|---|---|---|
| TB/NC group | POS | 0.145 | 0.971 | 0.917 |
| | NEG | 0.222 | 0.946 | 0.876 |
| TB/CAP group | POS | 0.137 | 0.877 | 0.666 |
| | NEG | 0.147 | 0.860 | 0.656 |
| TB/LC group | POS | 0.174 | 0.919 | 0.749 |
| | NEG | 0.163 | 0.910 | 0.703 |

POS, positive; NEG, negative; $R^2X$, the interpretability of the model for the categorical variable X; $R^2Y$, the interpretability of the model for the categorical variable Y ; $Q^2$ values , predictability of the model; TB: pulmonary tuberculosis; CAP: community acquired pneumonia; LC: lung cancer.

### *3.3. Metabolomics and bioinformatics analysis*

Furthermore, comprehensive analysis of metabolic pathways indicated that compared with the NC group, differentially abundant metabolites in the TB group were mainly enriched in aminoacyl-tRNA biosynthesis, primary bile acid biosynthesis, and purine metabolism. Interestingly, metabolic pathways over-represented by differentially abundant metabolites between the TB and CAP/LC groups were distinct from the TB group compared with the NC group. For instance, butanoate, phenylalanine, caffeine metabolism, citrate (TCA) cycle, alanine, aspartate, and glutamate metabolism were metabolic pathways outlined by the metabolite signature identified from the comparison between the TB and the CAP group; while nitrogen, tyrosine, vitamin B6 metabolism, ubiquinone and other terpenoid-quinone biosynthesis were unique pathways highlighted by differentially abundant

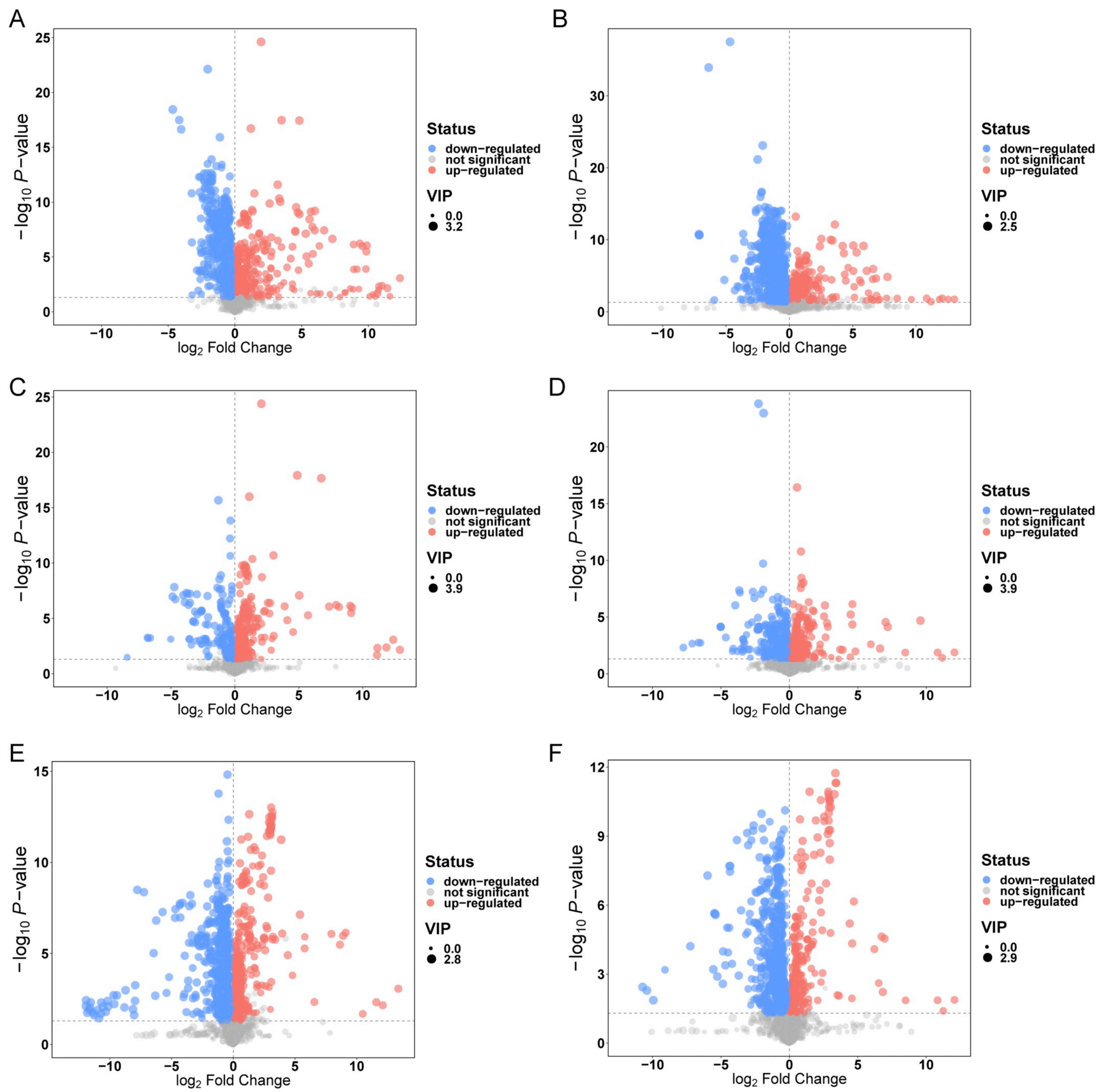


**Fig. 2.** Volcanic map of differential metabolites. For the TB/NC group in positive (A) and negative (B) ion mode, for the TB/CAP group in positive (C) and negative (D) ion mode, for the TB/LC group in positive (E) and negative (F) ion mode. The abscissa represented the fold change of the group compared to each substance (take the base 2 logarithm), the ordinate represented the P-value (take the base 10 logarithm), and the scatter size represented the VIP value of the OPLS-DA model. The larger the scattering, the larger the VIP value. The scatter color represented the final screening result. Significantly up-regulated metabolites are shown in red, significantly down-regulated metabolites are shown in blue, and non-significant differential metabolites are shown in gray. (For interpretation of the references to color in this figure legend, the reader is referred to the web version of this article.)

metabolites between the TB group and the LC group (Fig. 3).

### 3.4. Differentially abundant metabolites in pulmonary TB

Next, the abnormally abundant metabolites in the pulmonary TB compared with the other three groups were sought by studying all metabolites in the pulmonary TB group, the NC group, the CAP group, and the LC group. These differentially abundant metabolites had VIP > 1.2 and $P < 0.05$. Based on these criteria, three differential metabolites were identified, including Xanthine, 4-Pyridoxate, and D-glutamic acid (G-Glu) (Fig. 4). The plasma level of xanthine was significantly down-regulated in the pulmonary TB group compared with the NC group and the LC group, while the level of xanthine was significantly up-regulated in the pulmonary TB group compared with the CAP group. In addition, the plasma levels of 4-Pyridoxate and D-Glu were significantly down-regulated in the pulmonary TB group, compared with the NC, CAP, and LC groups.

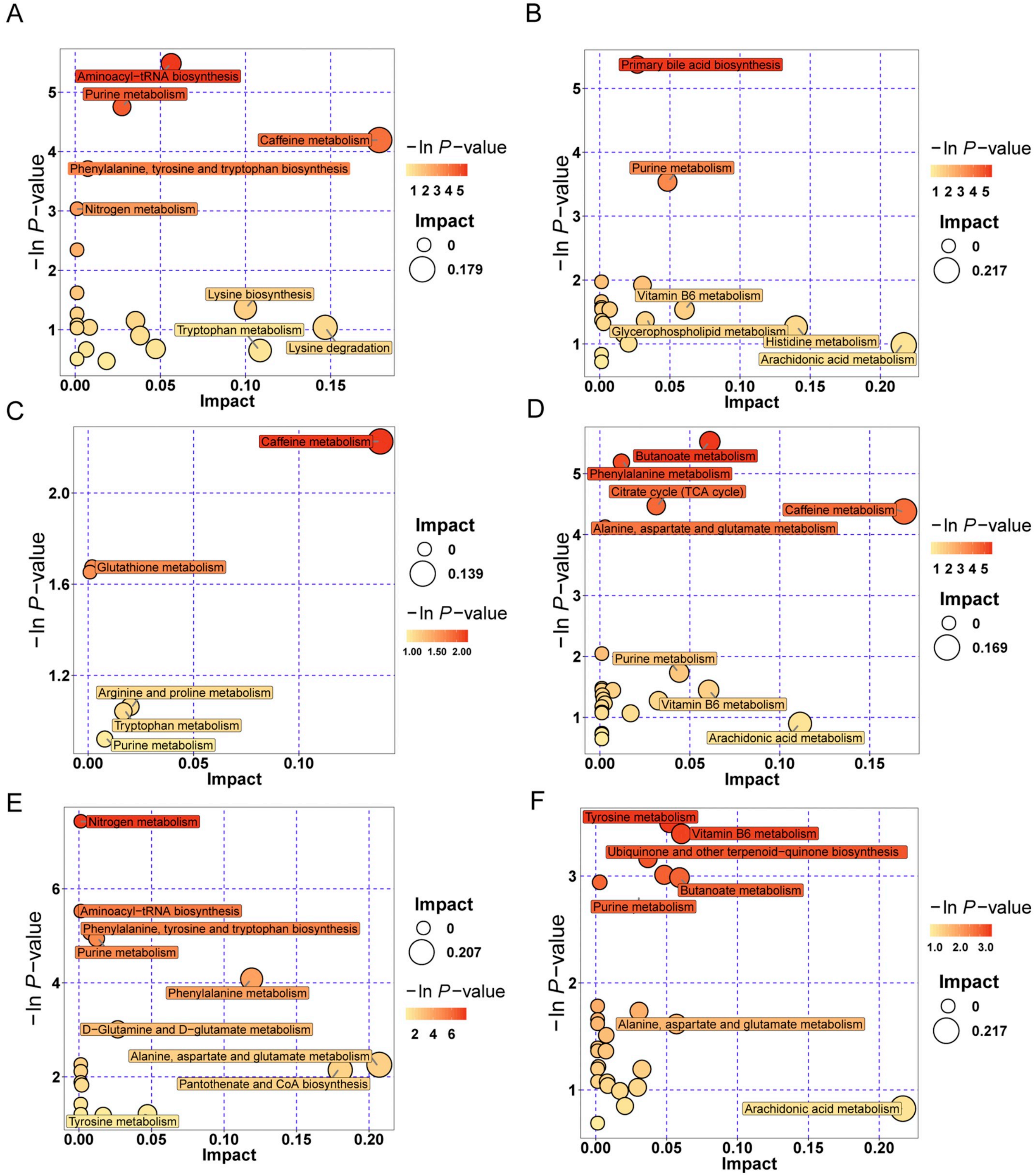


**Fig. 3.** Pathway analysis of differential metabolites. For the TB/NC group in positive (A) and negative (B) ion mode, for the TB/CAP group in positive (C) and negative (D) ion mode, for the TB/LC group in positive (E) and negative (F) ion mode.

## 4. Discussion

Pulmonary TB can be transmitted by droplet nuclei that contain the pathogen MTB through coughing, sneezing and talking [18]. However, it is estimated that delayed or misdiagnosis can occur in 10–50% of TB patients [19]. In a multicenter cross-sectional study from Iran, only 12.8% of patients were diagnosed with TB for the first time, and most of these patients eventually entered the TB treatment process through three or four physicians [20]. A survey from eastern province in China showed that 33.6% of TB patients could not receive timely medical treatment due to delayed diagnosis [21]. Therefore, screening the specific small molecule metabolites in the blood has potential to

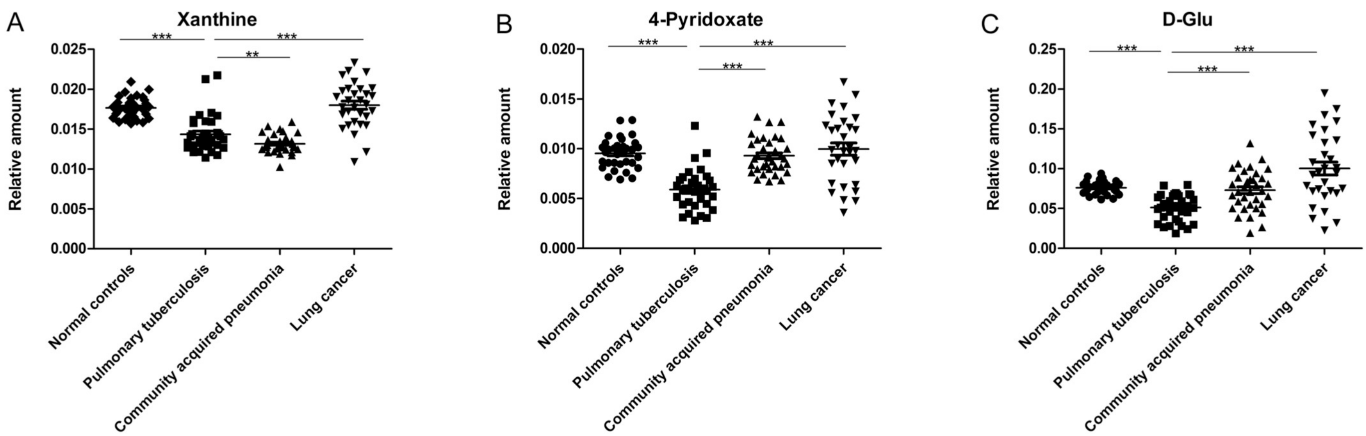


**Fig. 4.** Plasma relative quantification of three differential metabolites. Among TB patients (N = 35), CAP patients (N = 35), LC patients (N = 31) and normal controls (N = 35). Median values are shown by a horizontal line. P-values were calculated with Mann-Whitney U test. *$p < 0.05$, **$p < 0.01$, ***$p < 0.001$.

improve the diagnostic accuracy and may provide unified diagnostic criteria for pulmonary TB.

In this study, the pathway analysis indicated that TB is a consumptive disease, and the energy conversion process in human body is accelerated after MTB infection. Upon entry into macrophages, the major carbon and energy sources of MTB are transformed from carbohydrates to lipids [22]. And the intermediates of various amino acids and purine metabolism can participate in the nitrogen metabolism and remedial synthesis pathway of MTB [23–26]. Increased biosynthesis of ubiquinone and other terpenoid-quinone may not only serve as important hydrogen donor in the respiratory chain, but could also inhibit the activation of polymorphic neutrophils [10] and can down-regulate the level of superoxide in lipid beta oxidation [27]. Therefore, MTB could utilize the carbon and nitrogen sources in the host to maintain its own reproduction and virulence, and it may also imply one of the ways by which the host clears MTB. The metabolic changes in the blood of pulmonary TB patients may provide the basis for identifying potential biomarkers.

We identified three differentially abundant metabolites that were involved in the pathological process of pulmonary TB and can reflect the MTB pathogenicity. Hypoxanthine is catalyzed by xanthine oxidase (XO) to produce Xanthine [28]. MTB in macrophages relies on hypoxanthine-guanine phosphoribosyltransferase (HGPRT; EC 2.4.2.8) to recover hypoxanthine from the host for salvage synthesis pathways [29]. HGPRT has been shown to be a target for new anti-MTB drugs [30]. The down-regulation of Xanthine in the TB/NC group may be due to the consumption of upstream hypoxanthine by MTB in large quantities to synthesize the DNA. In cancer tissue, cells proliferate rapidly [31] and purine metabolism is stronger than TB, which is consistent with the results of our study. The level of xanthine in the TB/NC group and the CAP/NC group was down-regulated. However, the degree of decline in the CAP group was greater than the TB group, indicating that the level of xanthine in the TB group was higher than that of the CAP group. Xanthine has been shown to be a possible marker of hypoxia and an association with necrotic processes [32].Unlike pulmonary TB, the lung tissue destruction in acute inflammatory pneumonia is faster and severe. During pneumonia, a large amount of xanthine may enter the blood stream in a short period of time and is decomposed by XO enzyme. However, in the present study, no significant difference was observed in the final product (uric acid) in each group, which may be due to the purine nucleotide repair pathway in the body [33]. Because Xanthine is closely related to the reproduction of MTB, it may reflect the amount of MTB in the body and could predict the severity of TB infection in the lungs.

4-Pyridoxate is a decomposition product of vitamin B6. In the body fluid circulation, vitamin B6 is mainly present in the active form of pyridoxal-5′-phosphate (PLP) [34]. Dick T et al. found that MTB can directly synthesize PLP using host vitamin B6. It has also been demonstrated in the Δpdx1 mutant mouse model that MTB lacking PLP could not cause any significant pathological damage in the lung [35]. In this study, the level of 4-Pyridoxate was decreased in the TB group, compared with the non-TB groups. It may be due to the utilization of a large amount of vitamin B6 by MTB to maintain its own replication and virulence. In addition, the lack of vitamin B6 in the body can reduce the number of blood lymphocytes, especially T helper (Th) cells [36]. However, specific Th1 responses are critical for MTB control [37]. Therefore, the consumption of vitamin B6 by MTB in large quantity may affect the normal function of human cellular immunity and indulge the spread of TB. So, 4-Pyridoxate may reflect the virulence of MTB, and could predict the extent of pathological damage in the body after MTB infection.

D-Glu is derived from food intake in humans. Since the human body cannot decompose and utilize D-Glu, free D-Glu is present in tissue fluid at a surprisingly high level [38]. The peptidoglycan (PGN) is the major constituent of the MTB cell wall and contains the specific structure of amidated free carboxylic acid of D-Glu. In this study, the level of D-Glu in the TB group was significantly lower than that of the non-TB groups. D-Glu, which is amidated in the PGN peptide of MTB, has been reported to strongly reduce the activation of the human nucleotide-binding oligomerization domain-containing protein 1 (NOD1) [39]. NOD1 is an intracellular pattern recognition receptor, which can recognize PGN and activates macrophages to produce large amounts of tumor necrosis factor (TNF), interleukin (IL)-6 and IL-1β [40,41]. Therefore, consumption of a large amount of D-Glu may also be a key factor for MTB to avoid host sterilization. D-Glu may be associated with the severity of TB infection and could suggest the change in the body's immunity to MTB.

In conclusion, we identified three differential plasma metabolites that underwent significant changes after MTB infection. Given the role of these three metabolites in the pulmonary TB group, we hypothesized that MTB could potentially consume energy through multiple pathways in order to maintain its own reproduction and virulence. These metabolites may reflect the severity of MTB infection in patients with TB and the strength of the body's immune defense. Therefore, Xanthine, 4-Pyridoxate and D-Glu may serve as potential biomarkers for pulmonary TB. The present study provided experimental data for developing laboratory standards for potential biomarkers of pulmonary TB.

Supplementary data to this article can be found online at https://doi.org/10.1016/j.cca.2019.08.017.

## Funding

This work was supported by grants from the National Natural Science Foundation of China (81573709, 81772266), and Natural Science Foundation of Guangdong Province (2017A030311014), and

Guangzhou Science and Technology Project (201804010369).

## Authors' contributions

JCL contributed to the research design. HH and WJY performed the experiments. HH and YSH were in charge of figures. LYS, LLW, ZWP, HH, JC, TTJ, ZBL, HHT and YTH performed the collection of plasma samples and subjects' clinical data. JCL and HH coordinated the data modeling and wrote the manuscript. All authors had reviewed and approved the manuscript.

## Dataset

This data is available at the NIH Common Fund's Metabolomics Data Repository and Coordinating Center (supported by NIH grant, U01-DK097430) website, the Metabolomics Workbench, http://www.metabolomicsworkbench.org, where it has been assigned Project ID PR000824. The data can be accessed directly via it's Project DOI: 10.21228/M85Q5K.

## Declaration of Competing Interest

None declared.

## Acknowledgements

We thank all the subjects enrolled in the study, and we also thank Hong-Bin Zhou at the Zhejiang People's Hospital for collecting blood samples.

## References

[1] World Health Organization, Global Tuberculosis Report 2018, World Health Organization Web Site, 2018 http://www.who.int/tb/publications/global_report/en/ , Accessed date: 30 October 2018.
[2] M.A. Espinal, M.C. Raviglione, R. Gupta, Tuberculosis as a major global health problem in the 21st century: a WHO perspective, Semin. Respir. Crit. Care Med. 25 (2004) 245–253, https://doi.org/10.1055/s-2004-829520.
[3] A.D. Harries, A.M.V. Kumar, Challenges and progress with diagnosing pulmonary tuberculosis in low- and middle-income countries, Diagnostics 8 (2018) 78, https://doi.org/10.3390/diagnostics8040078.
[4] S.E. Dorman, S.G. Schumacher, D. Alland, et al., Xpert MTB/RIF ultra for detection of, Mycobacterium tuberculosis, and rifampicin resistance: a prospective multicentre diagnostic accuracy study, Lancet Infect. Dis. 18 (2018) 76–84, https://doi.org/10.1016/S1473-3099(17)30691-6.
[5] J.M. Cliff, S.H. Kaufmann, H. McShane, et al., The human immune response to tuberculosis and its treatment: a view from the blood, Immunol. Rev. 264 (2015) 88–102, https://doi.org/10.1111/imr.12269.
[6] A.B. Hodgson, R.K. Randell, T.K. Mahabir-Jagessar, et al., Acute effects of green tea extract intake on exogenous and endogenous metabolites in human plasma, J. Agric. Food Chem. 62 (2014) 1198–1208, https://doi.org/10.1021/jf404872y.
[7] Richard D. Beger, Warwick Dunn, Michael A. Schmidt, et al., Metabolomics enables precision medicine: "a white paper, community perspective", Metabolomics 12 (2016) 149 (doi:10.1007%2Fs11306-016-1094-6).
[8] J. Weiner 3rd, S.K. Parida, J. Maertzdorf, et al., Biomarkers of inflammation, immunosuppression and stress with active disease are revealed by metabolomic profiling of tuberculosis patients, PLoS ONE 7 (2012) e40221, , https://doi.org/10.1371/journal.pone.0040221.
[9] A. Zhou, J. Ni, Z. Xu, et al., Application of 1H NMR spectroscopy-based metabolomics to sera of tuberculosis patients, J. Proteome Res. 12 (2013) 4642–4649, https://doi.org/10.1021/pr4007359.
[10] S. Feng, Y.Q. Du, L. Zhang, et al., Analysis of serum metabolic profile by ultra-performance liquid chromatography-mass spectrometry for biomarkers discovery: application in a pilot study to discriminate patients with tuberculosis, Chin. Med. J. 128 (2015) 159–168, https://doi.org/10.4103/0366-6999.149188.
[11] Jiyan Liu, Tingting Jiang, Liliang Wei, et al., The discovery and identification of a candidate proteomic biomarker of active tuberculosis, BMC Infect. Dis. (2013) 506–516, https://doi.org/10.1186/1471-2334-13-506.
[12] S.K. Lau, K.C. Lee, S.O. Curreem, et al., Metabolomic profiling of plasma from patients with tuberculosis using untargeted mass spectrometry reveals novel biomarkers for diagnosis, J. Clin. Microbiol. 53 (2015) 3750–3759, https://doi.org/10.1128/JCM.01568-15.
[13] National Health Commission of the People's Republic of China, Diagnostic Criteria for Pulmonary Tuberculosis, http://www.nhc.gov.cn/ewebeditor/uploadfile/2017/12/20171212154852389.pdf (accessed Nov 09 2017).
[14] Chinese Medical Association, Chinese Medical Journals Publishing House, Chinese Society of General Practice, et al., Guideline for primary care of adult community acquired pneumonia, Chin. J. Gen. Pract. 18 (2) (2019) 117–126 (In Chinese), http://zhqkyszz.yiigle.com/CN114798201902/1116963.htm?locale=zh_CN.
[15] W.B. Dunn, D. Broadhurst, P. Begley, et al., Procedures for large-scale metabolic profiling of serum and plasma using gas chromatography and liquid chromatography coupled to mass spectrometry, Nat. Protoc. 6 (2011) 1060–1083, https://doi.org/10.1039/b418288j.
[16] J. Wang, T. Zhang, X. Shen, et al., Serum metabolomics for early diagnosis of esophageal squamous cell carcinoma by UHPLC-QTOF/MS, Metabolomics 12 (2016) 116, https://doi.org/10.1038/nprot.2011.335.
[17] C.A. Smith, E.J. Want, G. O'Maille, et al., XCMS: processing mass spectrometry data for metabolite profiling using nonlinear peak alignment, matching, and identification, Anal. Chem. 78 (2006) 779–787, https://doi.org/10.1021/ac051437y.
[18] G. Churchyard, P. Kim, N.S. Shah, et al., What we know about tuberculosis transmission: an overview, J. Infect. Dis. 216 (2017) S629–S635, https://doi.org/10.1093/infdis/jix362.
[19] M.L. Graber, The incidence of diagnostic error in medicine, BMJ Qual. Saf. 22 (2013) 21–27, https://doi.org/10.1136/bmjqs-2012-001615.
[20] T.B. Khoo, J.W. Tan, H.P. Ng, et al., Paediatric in-patient prescribing errors in Malaysia: a cross-sectional multicentre study, Int. J. Clin. Pharm. 39 (2017) 551–559, https://doi.org/10.1007/s11096-017-0463-1.
[21] X.H. Fang, H.H. Shen, W.Q. Hu, et al., Prevalence of and factors influencing anti-tuberculosis treatment non-adherence among patients with pulmonary tuberculosis: a cross-sectional study in Anhui Province, eastern China, Med. Sci. Monit. 25 (2019) 1928–1935, https://doi.org/10.12659/MSM.913510.
[22] M.A. Forrellad, M. McNeil, L. Santangelo Mde, et al., Role of the Mce1 transporter in the lipid homeostasis of Mycobacterium tuberculosis, Tuberculosis 94 (2014) 170–177, https://doi.org/10.1007/s11096-017-0463-1.
[23] B.S. Somashekar, A.G. Amin, P. Tripathi, et al., Metabolomic signatures in Guinea pigs infected with epidemic-associated W-Beijing strains of Mycobacterium tuberculosis, J. Proteome Res. 11 (2012) 4873–4884, https://doi.org/10.1021/pr300345x.
[24] J.H. Shin, J.Y. Yang, B.Y. Jeon, et al., (1)H NMR-based metabolomic profiling in mice infected with Mycobacterium tuberculosis, J. Proteome Res. 10 (2011) 2238–2247, https://doi.org/10.1021/pr101054m.
[25] L. Luier, D.T. Loots, Tuberculosis metabolomics reveals adaptations of man and microbe in order to outcompete and survive, Metabolomics 12 (2016) 40, https://doi.org/10.1007/s11306-016-0969-x.
[26] W.B. Parker, M.C. Long, Purine metabolism in Mycobacterium tuberculosis as a target for drug development, Curr. Pharm. Des. 13 (2007) 599–608, https://doi.org/10.2174/138161207780162863.
[27] S. Agrawal, K. Jaswal, A.L. Shiver, et al., A genome-wide screen in Escherichia coli reveals that ubiquinone is a key antioxidant for metabolism of long-chain fatty acids, J. Biol. Chem. 292 (2017) 20086–20099, https://doi.org/10.1074/jbc.M117.806240.
[28] Y.J. Kim, H.M. Ryu, J.Y. Choi, et al., Hypoxanthine causes endothelial dysfunction through oxidative stress-induced apoptosis, Biochem. Biophys. Res. Commun. 482 (2017) 821–827, https://doi.org/10.1016/j.bbrc.2016.11.119.
[29] G. Biazus, C.Z. Schneider, M.S. Palma, et al., Hypoxanthine-guanine phosphoribosyltransferase from Mycobacterium tuberculosis H37Rv: cloning, expression, and biochemical characterization, Protein Expr. Purif. 66 (2009) 185–190, https://doi.org/10.1016/j.pep.2009.04.001.
[30] W.S. Eng, D. Rejman, R. Pohl, et al., Pyrrolidine nucleoside bisphosphonates as antituberculosis agents targeting hypoxanthine-guanine phosphoribosyltransferase, Eur. J. Med. Chem. 159 (2018) 10–22, https://doi.org/10.1016/j.ejmech.2018.09.039.
[31] M. Garcia-Gil, M. Camici, S. Allegrini, et al., Emerging role of purine metabolizing enzymes in brain function and tumors, Int. J. Mol. Sci. 19 (2018) 3598, https://doi.org/10.3390/ijms19113598.
[32] J.R. Wu, J.H. Hsu, Z.K. Dai, et al., Activation of endothelial NO synthase by a xanthine derivative ameliorates hypoxia-induced apoptosis in endothelial progenitor cells, J. Pharm. Pharmacol. 68 (2016) 810–818, https://doi.org/10.1111/jphp.12555.
[33] A. Rodríguez-Núñez, F. Camiña, S. Lojo, et al., Concentrations of nucleotides, nucleosides, purine bases and urate in cerebrospinal fluid of children with meningitis, Acta Paediatr. 82 (1993) 849–852, https://doi.org/10.1111/j.1651-2227.1993.tb12577.x.
[34] P. Zhang, K. Tsuchiya, T. Kinoshita, et al., Vitamin B6 prevents IL-1β production by inhibiting NLRP3 inflammasome activation, J. Biol. Chem. 291 (2016) 24517–24527, https://doi.org/10.1074/jbc.M116.743815.
[35] T. Dick, U. Manjunatha, B. Kappes, et al., Vitamin B6 biosynthesis is essential for survival and virulence of Mycobacterium tuberculosis, Mol. Microbiol. 78 (2010) 980–988, https://doi.org/10.1111/j.1365-2958.2010.07381.x.
[36] P.M. Ueland, A. McCann, Ø. Midttun, et al., Inflammation, vitamin B6 and related pathways[J], Mol. Asp. Med. 53 (2017) 10–27, https://doi.org/10.1016/j.mam.2016.08.001.
[37] L.D. Jasenosky, T.J. Scriba, W.A. Hanekom, et al., Immunol. Rev. 264 (2015) 74–87, https://doi.org/10.1111/imr.12274.
[38] Human Metabolome Database, Showing Metabocard for D-Glutamic Acid (HMDB0003339), http://www.hmdb.ca/metabolites/HMDB0003339 (accessed Jan 11 2019).
[39] Q. Wang, Y. Matsuo, A.R. Pradipta, et al., Synthesis of characteristic Mycobacterium peptidoglycan (PGN) fragments utilizing with chemoenzymatic preparation of meso-diaminopimelic acid (DAP), and their modulation of innate immune responses, Org. Biomol. Chem. 14 (2016) 1013–1023, https://doi.org/10.1039/c5ob02145f.
[40] S. Vijayrajratnam, A.C. Pushkaran, A. Balakrishnan, et al., Bacterial peptidoglycan with amidated meso-diaminopimelic acid evades NOD1 recognition: an insight into NOD1 structure-recognition, Biochem. J. 473 (2016) 4573–4592, https://doi.org/10.1042/BCJ20160817.
[41] M.V. Pashenkov, L.S. Balyasova, Y.A. Dagil, et al., The role of the p38–MNK–eIF4E signaling axis in TNF production downstream of the NOD1 receptor, J. Immunol. 198 (2017) 1638–1648, https://doi.org/10.4049/jimmunol.1600467.